

# Escape from bounded domains driven by multi-variate $\alpha$ -stable noises

Krzysztof Szczepaniec<sup>1,\*</sup> and Bartłomiej Dybiec<sup>1,†</sup>

<sup>1</sup>*Marian Smoluchowski Institute of Physics, and Mark Kac Center for Complex Systems Research,  
Jagiellonian University, ul. Reymonta 4, 30-059 Kraków, Poland*

(Dated: August 8, 2022)

In this paper we provide an analysis of a mean first passage time problem of a random walker subject to a bi-variate  $\alpha$ -stable Lévy type noise from a 2-dimensional disk. We analyze the case for an arbitrary absorbing arc, defined by an angle parameter  $\phi$ , from small values, up to a limiting case of the full angle  $\phi = 2\pi$  where the entire disk edge is absorbing. For an appropriate choice of parameters the mean first passage time reveals non-monotonous dependence on the stability index  $\alpha$  describing jumps' length asymptotics. Finally, we study escape from  $d$ -dimensional hyper-sphere and hyper-cube showing that  $d$ -dimensional escape process can be used to discriminate between various types of multi-variate  $\alpha$ -stable noises.

PACS numbers: 05.40.Fb, 05.10.Gg, 02.50.-r, 02.50.Ey,

## I. INTRODUCTION

Models of random walks [1–4] hold a vital place in statistical physics as an analysis tool for large amount of physical systems [5–10]. The canonical, well understood, Brownian motion still plays the major role, however various non-Gaussian and non-Markovian generalizations have been introduced. Heavy tailed fluctuation have been observed in versatilities of models [11–14] including physics, chemistry or biology [15, 16], paleoclimatology [17] or economics [18] and epidemiology [19, 20] to name a few. Observations of the so-called Lévy flights boosted the theory of random walks and noise induced phenomena into new directions [21–28] which involve examination of space fractional diffusion equation (Smoluchowski-Fokker-Planck equation) and stimulated development of more general theory [29, 30]. Theory of  $\alpha$ -stable processes allows for examination of more general fluctuations than Gaussian including them as a limiting case. The high efficiency and generality of  $\alpha$ -stable processes is based on the generalized central limit theorem, which provides extension of the standard central limit theorem to the situation when assumption of finite variance of elements is relaxed. Consequently,  $\alpha$ -stable processes provide natural tool for description of systems revealing power-law fluctuations.

The problem of noise-induced escape from finite intervals, with the canonical example of one-dimensional diffusion, has been studied in great details in various non-Gaussian and non-Markovian [31–33] regimes including  $\alpha$ -stable Lévy type noise as an especially important extension. Analysis of the mean first passage time (escape time) from a finite interval provides an insight into the complexity of stable noise. The interplay of noise parameters and non-locality of boundary conditions [32, 34] result in reach behavior of  $\alpha$ -stable noise driven systems. In particular, their non-triviality is manifested in a non-linear, non-monotonous behavior of the mean first passage time which measures efficiency of the noise facilitated escape.

So far majority of research focuses mainly on uni-variate processes. Extensions into multi-variate domains seem natural, yet still challenging due to their non-triviality. General approach to 2-dimensional Lévy flights assume that a step direction is chosen from uniform distribution on a circle and jumps' lengths are distributed according to heavy-tailed densities. Such approach leads to desired Lévy flights, providing effective model for various different processes [35]. Nevertheless, an alternative and natural approach based on bi-variate  $\alpha$ -stable distributions has been suggested [36]. In such a case, on the one hand, the whole process is determined by a multi-variate  $\alpha$ -stable density which contains all the information about increments of the process. On the other hand plenitude of possible spectral measures, leading to various (fractional) diffusion equations, shifts the main difficulties into a different place.

In this paper we explore a 2-dimensional escape problem, with a random walker driven by a bi-variate Lévy stable noise which provides a natural, yet non-trivial, extension of 1D  $\alpha$ -stable noises to higher dimensions. Starting from known results for 1D escape problem, with the non-monotonous dependence of the mean first passage time as a function of the stability index  $\alpha$ , see [32, 34], we search for analogous behavior in the noise driven escape process from a disk. Finally, we discuss the problem of independence of increments of multi-variate  $\alpha$ -stable motions in the context of the escape from  $d$ -dimensional hyper-cube and order statistics.

## II. MODEL AND RESULTS

As a starting point, we recall the problem of the noise driven escape from a finite 1D interval (Sec. II A), which is also used to present applied methods and basic theory. Next, the 2D case, i.e. the noise induced escape from a disk, is discussed (Sec. II B). We analyze various cases of absorbing edge, given by an angle parameter  $\phi \in (0, 2\pi]$ . Finally, general problems of escape from  $d$ -dimensional (Sec. II C) hyper-sphere (Sec. II C 1) and hyper-cube (Sec. II C 2) are studied.

\*Electronic address: kszczepaniec@th.if.uj.edu.pl

†Electronic address: bartek@th.if.uj.edu.pl

### A. 1D motivation

A motion of a free particle subject to the  $\alpha$ -stable Lévy type noise is described by the following Langevin equation

$$\frac{dx}{dt} = \sigma \zeta_{\alpha,0}(t), \quad (1)$$

which can be rewritten as

$$dx = \sigma dL_{\alpha,0}(t), \quad (2)$$

where  $L_{\alpha,0}(t)$  is a symmetric  $\alpha$ -stable motion [37] i.e. stochastic process with independent increments distributed according to an  $\alpha$ -stable density [30, 37].  $\zeta_{\alpha,0}(t)$  represents a white  $\alpha$ -stable noise which is a formal time derivative of a symmetric  $\alpha$ -stable motion. The characteristic function of  $\alpha$ -stable densities is given by the following formula [29, 30]

$$\phi(k) = \mathbb{E} \left[ e^{ikX} \right] = \begin{cases} \exp \left[ -\sigma^\alpha |k|^\alpha \left( 1 - i\beta \text{sign} k \tan \frac{\pi\alpha}{2} \right) + i\mu k \right] & \text{if } \alpha \neq 1, \\ \exp \left[ -\sigma |k| \left( 1 + i\beta \frac{2}{\pi} \text{sign} k \ln |k| \right) + i\mu k \right] & \text{if } \alpha = 1, \end{cases} \quad (3)$$

where  $\alpha \in (0, 2]$  is the stability index,  $\beta \in [-1, 1]$  is the asymmetry (skewness) parameter,  $\sigma > 0$  is the scale parameter and finally  $\mu \in \mathbb{R}$  is the location parameter. For  $\alpha < 2$ , symmetric  $\alpha$ -stable densities, i.e. ones with  $\beta = 0$ , have the power-law asymptotics of  $|x|^{-(\alpha+1)}$  type.

In 1D, Eq. (1) can be associated with the following (space-fractional) Smoluchowski-Fokker-Planck equation [23, 38–41]

$$\frac{\partial p(x, t|x_0, 0)}{\partial t} = \sigma^\alpha \frac{\partial^\alpha p(x, t|x_0, 0)}{\partial |x|^\alpha}. \quad (4)$$

In the above equation the Riesz-Weyl fractional derivative is defined by the Fourier transform, i.e.  $\mathcal{F} \left[ \frac{\partial^\alpha f(x)}{\partial |x|^\alpha} \right] = -|k|^\alpha \mathcal{F} [f(x)]$ . For  $\alpha = 2$ , any Lévy stable noise is equivalent to the Gaussian white noise (with the intensity  $\sqrt{2}\sigma$ , see [29]) and the fractional Smoluchowski-Fokker-Planck equation (4) takes its standard form, i.e.  $\partial^\alpha / \partial |x|^\alpha \rightarrow \partial^2 / \partial x^2$ .

Motion of the particle can be restricted by geometric constraints which introduce boundary conditions. For example, a domain of motion can be a finite  $[-L, L]$  interval restricted by two absorbing boundaries. Presence of absorbing boundaries require special care. In particular, for  $\alpha < 2$ , trajectories of  $\alpha$ -stable motions are discontinuous. Consequently, for  $\alpha < 2$ , fractional Smoluchowski-Fokker-Planck equation is associated with the non-local boundary conditions, i.e.  $p(x, t|x_0, 0) = 0$  for  $|x| \geq L$ , see [32, 34]. In the Gaussian case ( $\alpha = 2$ ) boundary conditions are local (defined at  $|x| = L$  only) and the solution of Eq. (4) can be constructed using Fourier series [42, Eq. (81)] and for  $x_0 = 0$ , it reads

$$p(x, t|0, 0) = \sum_{n=1}^{\infty} \frac{1}{L} \sin \left[ \frac{n\pi}{2} \right] \sin \left[ \frac{n\pi(x+L)}{2L} \right] \exp \left[ -\frac{n^2\pi^2\sigma^2}{4L^2} t \right]. \quad (5)$$

From Eq. (5) one can calculate the survival probability  $S(t) = \int_{-L}^L p(x, t|0, 0) dt$

$$S(t) = \sum_{n=1}^{\infty} \frac{4}{n\pi} \sin^3 \left[ \frac{n\pi}{2} \right] \exp \left[ -\frac{n^2\pi^2\sigma^2}{4L^2} t \right], \quad (6)$$

which gives the probability that at time  $t$  a random walker is still in the  $[-L, L]$  interval. From the survival probability the first passage time density  $f(t)$  can be calculated

$$f(t) = -\frac{dS}{dt} = \sum_{n=1}^{\infty} \frac{n\pi\sigma^2}{L^2} \sin^3 \left[ \frac{n\pi}{2} \right] \exp \left[ -\frac{n^2\pi^2\sigma^2}{4L^2} t \right]. \quad (7)$$

The first passage time density has the exponential asymptotics determined by the lowest eigenvalue, see Eq. (7), and the mean first passage time  $\mathcal{T} = \langle \tau \rangle$  from a bounded interval is finite

$$\mathcal{T} = \langle \tau \rangle = \int_0^{\infty} f(t) t dt = \frac{L^2}{2\sigma^2} = \frac{L^2}{\Gamma(2+1)\sigma^2}. \quad (8)$$

The mean first passage time (MFPT) is the average time which is needed to cross the (absorbing) boundary. The exact value of the MFPT depends on the initial position. Here, it is assumed that initially a test particle is located in the center of the domain of motion (interval).

Alternatively, the average earliest time  $\mathcal{T} = \langle \tau \rangle$ , see Eq. (8), at which a particle leaves the region  $\Omega = [-L, L]$  for the first time can be directly calculated from the backward Smoluchowski-Fokker-Planck equation [43]

$$\sigma^2 \frac{\partial^2 \mathcal{T}(x)}{\partial x^2} = \sigma^2 \nabla^2 \mathcal{T}(x) = -1, \quad (9)$$

with the boundary condition  $\mathcal{T}|_{\partial\Omega} = 0$  and the initial condition  $x(0) \in \Omega$ . For  $d = 1$ , the MFPT calculated from Eq. (9) is given by Eq. (8). Eq. (9) can be easily generalized to the fractional case [32]

$$\sigma^\alpha \frac{\partial^\alpha \mathcal{T}(x)}{\partial |x|^\alpha} = -1, \quad (10)$$

or into higher dimensions.

The mean first passage time for the escape from a finite interval  $[-L, L]$  restricted by two absorbing boundaries ( $x(0) = 0$ ) can be calculated for any value of the stability index  $\alpha$  [32]

$$\mathcal{T} = \langle \tau \rangle = \frac{L^\alpha}{\Gamma(1+\alpha)\sigma^\alpha}. \quad (11)$$

The extrema of  $\mathcal{T} = \langle \tau \rangle$  as a function of the stability index  $\alpha$  can be at boundaries of the stability index range ( $0 < \alpha \leq 2$ ). Nevertheless, the most interesting is the possibility of observing maximal value of the MFPT for an intermediate  $\alpha$ . Differentiating Eq. (11) with respect to  $\alpha$  gets

$$\ln L - \ln \sigma - \frac{d \ln \Gamma(1+\alpha)}{d\alpha} = \ln L - \ln \sigma - \psi_1(1+\alpha) = 0 \quad (12)$$

where  $\psi_1(1+\alpha) = \frac{d \ln \Gamma(1+\alpha)}{d\alpha}$  is a PolyGamma function. MFPT for  $\alpha$  given by Eq. (12) has maximum, because  $\frac{d^2 \mathcal{T}}{d\alpha^2}$  is negative at this point.

For  $\alpha \in (0, 2]$  PolyGamma can be approximated by the following fit

$$\psi_1(1+\alpha) \approx 1.044 \ln(0.574 + 0.923\alpha). \quad (13)$$

Using approximation (13) it is possible to find a relation between the interval half-width  $L$  and the scale parameter  $\sigma$  for which the maximal MFPT is recorded at given (fixed)  $\alpha$ . For example, assuming that the MFPT is maximal for  $\alpha = 1$  one approximately gets

$$\sigma \approx 0.656L \quad \text{or} \quad L \approx 1.523\sigma. \quad (14)$$

This demonstrates that for a given scale parameter  $\sigma$  it is possible to find such an interval half-width  $L$  that the MFPT depends in a non-monotonous way on the stability index  $\alpha$ . Alternatively, for a given  $L$  it is possible to find  $\sigma$  resulting in the minimal MFPT. In particular, using Eqs. (11) and (14)  $\mathcal{T} = \langle \tau \rangle = [\Gamma(1 + \alpha)0.656^\alpha]^{-1}$ , which has pronounced global maximum at  $\alpha \approx 1$ .

### B. Escape in 2D

Let us consider a 2D motion of a free overdamped particle subject to the bi-variate  $\alpha$ -stable Lévy type noise

$$\frac{d\mathbf{x}}{dt} = \sigma \zeta_\alpha(t). \quad (15)$$

where  $\langle \mathbf{k}, \mathbf{s} \rangle$  represents the scalar product,  $\Gamma(\cdot)$  stands for the spectral measure on the unit sphere  $S_d$  of  $\mathbb{R}^d$  and  $\boldsymbol{\mu}^0$  is a vector in  $\mathbb{R}^d$ , see [30]. Bi-variate case corresponds to  $d = 2$ . The spectral measure  $\Gamma(\cdot)$  replaces skewness and scale parameters ( $\beta$  and  $\sigma$ ) which characterize 1D  $\alpha$ -stable densities. Multi-variate  $\alpha$ -stable density is said to be symmetric if the spectral measure is symmetric, see [30, 36, 44]. The multi-variate  $\alpha$ -stable motion  $\mathbf{L}_\alpha(t)$  can be generated in analogous way like  $L_{\alpha,0}(t)$ , see [29, 45, 46]. The only difference is that the approximation scheme relies on generation of multi-variate  $\alpha$ -stable random variables, which can be generated by general methods described in [30, 47].

The 2D case significantly differs from 1D, because bi-variate  $\alpha$  stable noises are determined by the spectral measure  $\Gamma(\cdot)$ . Various choices of spectral measures result in different escape scenarios and different (fractional) diffusion equations. Here, we focus on the uniform continuous spectral measures, however, also discrete spectral measures concentrated on the intersection of the unit circle (or hyper-sphere) with axes are possible [13, 30, 48]. The uniform spectral measure  $\Gamma(\cdot)$  corresponds to the situation when  $\alpha$ -stable densities are spherically symmetric, i.e. their isolines are circles ( $d = 2$ ), spheres ( $d = 3$ ) or hyper-spheres ( $d > 3$ ). In such a case the Langevin equation (15) is associated with the following fractional dif-

Eq. (15) can be rewritten as

$$d\mathbf{x} = \sigma d\mathbf{L}_\alpha(t), \quad (16)$$

where  $\mathbf{L}_\alpha(t)$  is a symmetric, bi-variate  $\alpha$ -stable motion [30]. As in 1D, the bi-variate  $\alpha$ -stable noise is a formal time derivative of the bi-variate  $\alpha$ -stable motion. Therefore, increments of  $\mathbf{L}_\alpha(t)$  are independent and distributed according to bi-variate  $\alpha$ -stable density, which has the characteristic function

$$\phi(\mathbf{k}) = \begin{cases} \exp \left\{ - \int_{S_d} |\langle \mathbf{k}, \mathbf{s} \rangle|^\alpha \left[ 1 - i \text{sign}(\langle \mathbf{k}, \mathbf{s} \rangle) \tan \frac{\pi\alpha}{2} \right] \Gamma(d\mathbf{s}) + i \langle \mathbf{k}, \boldsymbol{\mu}^0 \rangle \right\} & \text{for } \alpha \neq 1, \\ \exp \left\{ - \int_{S_d} |\langle \mathbf{k}, \mathbf{s} \rangle|^\alpha \left[ 1 + i \frac{2}{\pi} \text{sign}(\langle \mathbf{k}, \mathbf{s} \rangle) \ln(\langle \mathbf{k}, \mathbf{s} \rangle) \right] \Gamma(d\mathbf{s}) + i \langle \mathbf{k}, \boldsymbol{\mu}^0 \rangle \right\} & \text{for } \alpha = 1, \end{cases} \quad (17)$$

fusion equation

$$\frac{\partial p(\mathbf{x}, t | \mathbf{x}_0, t)}{\partial t} = -\sigma^\alpha (-\Delta)^{\alpha/2} p(\mathbf{x}, t | \mathbf{x}_0, t), \quad (18)$$

where  $-(-\Delta)^{\alpha/2}$  is the fractional Riesz-Weil derivative (laplacian) defined via its Fourier transform [49]

$$\mathcal{F} \left[ -(-\Delta)^{\alpha/2} p(\mathbf{x}, t | \mathbf{x}_0, t) \right] = -|\mathbf{k}|^\alpha \mathcal{F} [p(\mathbf{x}, t | \mathbf{x}_0, t)]. \quad (19)$$

The associated backward equation (10) transforms into multi-dimensional domain in the same manner. Analogously like in 1D, Eq. (18) is associated with the non-local boundary conditions.

This time as a finite domain of motion a disk of radius  $R$  is considered. The absorbing boundary is defined by the disk edge which can be (a) absorbing or alternatively (b) a part of the edge — given arc — is absorbing while the remaining part is reflecting [50, 51]. The main aim is to check if non-monotonous dependence of the MFPT on the stability index  $\alpha$  can be observed in (a) and (b) in analogous way like it was observed in 1D, see Eq. (11). In order to verify this hypothesis we use extensive numerical simulations. Main simulations were performed on a circle with radius  $R = 4$ , number of repetitions  $N = 10^6$  and the integration time step  $\Delta t = 10^{-2}$ .

Initially a random walker was located in the center of the disk, i.e.  $\mathbf{x}(0) = \mathbf{0}$ . The first passage time  $\tau$  is estimated as

$$\tau = \min\{t > 0 : \mathbf{x}(0) = \mathbf{0} \text{ and } \mathbf{x}(t) \notin \Omega\}, \quad (20)$$

where  $\Omega$  is the domain of motion, e.g. interval, disk, etc. The mean first passage time is the average first passage time  $\langle \tau \rangle$ .

For  $\alpha = 2$ , i.e. for the bi-variate Gaussian white noise, using Eq. (9) it is possible to calculate the mean first passage time  $\mathcal{T}$  which is the first escape time from the disk of radius  $R$ . Due to the system symmetry, the only relevant variable is the initial distance from the disk center  $r$ . Rewriting Eq. (9) in polar coordinates one gets

$$\frac{d^2 \mathcal{T}(r)}{dr^2} + \frac{1}{r} \frac{d\mathcal{T}(r)}{dr} = -\frac{1}{\sigma^2}, \quad (21)$$

with the boundary condition  $\mathcal{T}(R) = 0$ . The solution of Eq. (21) is

$$\mathcal{T}(r) = \frac{1}{4\sigma^2} [R^2 - r^2], \quad (22)$$

which for  $r = 0$  reduces to  $R^2/4\sigma^2$ , i.e. the MFPT from the disk of radius  $R$  is two times smaller than the MFPT from the interval of the half-width  $R$ .

For the disk with entire absorbing edge, case (a), the mean first passage time is the time in which random walker, starting at the center of the disk reaches or passes over the edge of the disk for the first time. While, in general the behavior of the MFPT depends on the noise parameters, it is possible to find such a range of noise intensity  $\sigma$  for which the MFPT becomes a non-monotonous function of the stability index  $\alpha$ . Also, the position of MFPT maxima shifts with the change in the scale parameter  $\sigma$ . Fig. 1 demonstrates dependence of the mean first passage time from the disk on the stability index  $\alpha$ . Various curves correspond to various values of the scale parameter  $\sigma$ .

Non-monotonous dependence of the mean first passage time is observed for quite narrow range of the scale parameter  $\sigma$ . With the increasing scale parameter the MFPT monotonically decreases as a function of the stability index  $\alpha$ . The behavior of the MFPT is a consequence of the interplay between the stability index  $\alpha$  and the scale parameter  $\sigma$ . The stability index  $\alpha$  not only controls the tail asymptotics of  $\alpha$ -stable densities but also affects its width, as measured by the inter quantile distance.

In the situation (b) when only a part of the disk edge is absorbing and the remaining part is reflecting it is also possible to find non-monotonous dependence of the mean first passage time on the stability index  $\alpha$ . The absorbing arc is defined by a single parameter  $\phi \in (0, 2\pi]$ , which measures the absorbing angle. For example when  $\phi = 2\pi$  the whole edge is absorbing, i.e. the case (a) is recovered. The non-monotonous dependence can be observed for every absorbing arc indicating non-trivial properties of the studied model. Fig. 2 presents results for  $\phi = \pi$ , i.e. half of the disk edge is absorbing and the remaining half is reflecting. Finally, Fig. 3 demonstrates results for a very narrow angle, i.e.  $\phi = \pi/20$ . In both cases non-monotonous dependence of MFPT on stability index  $\alpha$  is

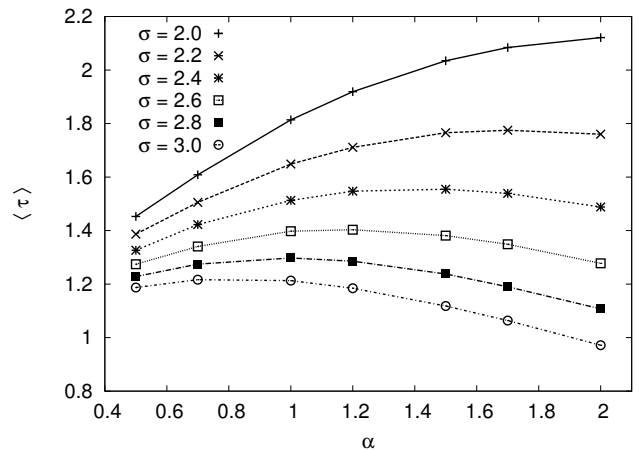


FIG. 1: The mean first passage time for the escape from the (2D) disk as a function of the stability index  $\alpha$ . The whole disk edge is absorbing. A particle starts its diffusive motion in the disk center. The disk radius is  $R = 4$ . Various curves correspond to various values of the scale parameter  $\sigma$ . Lines are drawn to guide the eye only.

clearly visible. With decreasing angle  $\phi$ , the MFPT increases see Figs. 1–3, what is the consequence of the fact that it is harder to escape from the disk when only a small part of the disk edge is absorbing [50, 51].

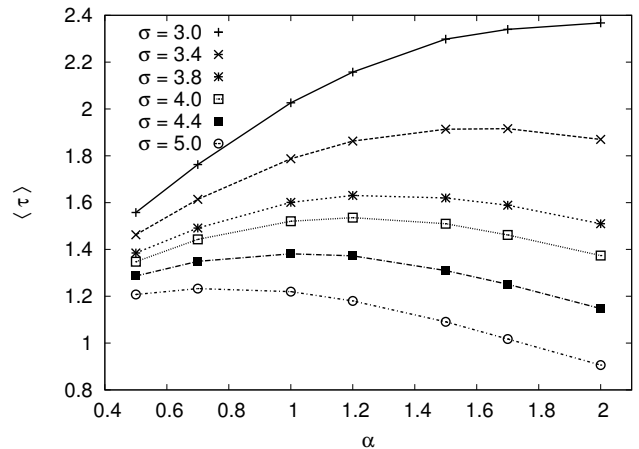


FIG. 2: The mean first passage time for the escape from the (2D) disk as a function of the stability index  $\alpha$ . The half of the disk edge is absorbing and the other half is reflecting. A particle starts its diffusive motion in the disk center. The disk radius is  $R = 4$ . Various curves correspond to various values of the scale parameter  $\sigma$ . Lines are drawn to guide the eye only. Error bars are smaller than the symbol size.

### C. Escape in $d$ -dimensions

In  $d$ -dimensions, escapes from the hyper-sphere and the hyper-cube are considered. Such a distinction is made in order to emphasize differences between both escape scenarios

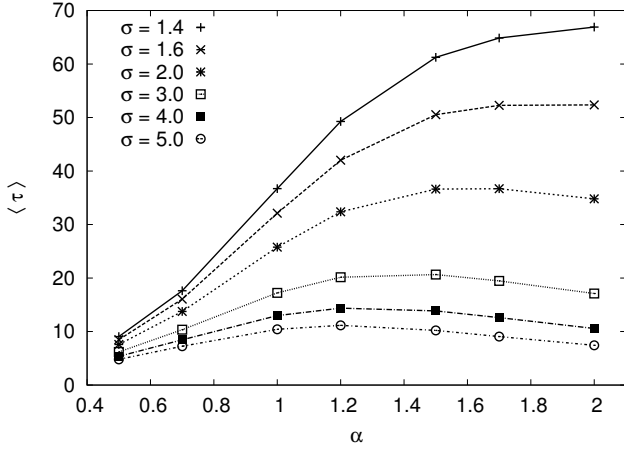


FIG. 3: The mean first passage time for the escape from the (2D) disk as a function of the stability index  $\alpha$ . The part of the disk edge ( $\pi/20$ ) is absorbing and the remaining part ( $39\pi/20$ ) is reflecting. A particle starts its diffusive motion in the disk center. The disk radius is  $R = 4$ . Various curves correspond to various values of the scale parameter  $\sigma$ . Lines are drawn to guide the eye only. Error bars are smaller than the symbol size.

and demonstrate how escape from the hyper-cube can be used to recognize some properties of underlying multi-variate  $\alpha$ -stable noises.

### 1. Hyper-sphere

For  $\alpha = 2$ , in  $d$ -dimensions, the MFPT can be calculated by use of Eq. (9), which in the polar coordinates takes the form

$$\mathcal{T}''(r) + \frac{d-1}{r}\mathcal{T}'(r) = -\frac{1}{\sigma^2} \quad (23)$$

and has the solution

$$\mathcal{T}(r) = \frac{1}{2\sigma^2 d} [R^2 - r^2], \quad (24)$$

which for  $r = 0$  reduces to  $R^2/d\sigma^2$ . For  $d = 3$  the sphere is reconstructed and the MFPT reads  $R^2/6\sigma^2$ , i.e. the MFPT from the sphere of radius  $R$  is three times smaller than the MFPT from the interval of half-width  $R$ . The solution (24) perfectly agrees with results of numerical simulations, see Fig. 4, where not only results of numerical simulations for  $\alpha = 2$  are presented but also theoretical values given by Eq. (24).

Figure 4 shows dependence of the mean first passage time on the dimension  $d$  of the hyper-sphere. Various curves correspond to various values of the stability index  $\alpha$ . From simulations, see top panel of Fig. 4, it looks that for the hyper-sphere

$$\mathcal{T} \propto \frac{1}{d^{\alpha/2}}. \quad (25)$$

This type of scaling can be deduced from the following reasoning. First, let us recall some properties of 1D  $\alpha$ -stable densities. Lévy distribution (with  $\alpha < 2$ ) are characterized by the

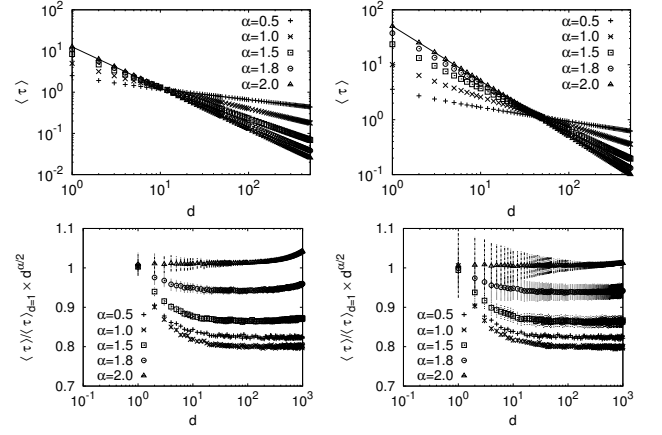


FIG. 4: The mean first passage times  $\langle \tau \rangle$  for the escape from the  $d$ -dimensional hyper-sphere (top row) and ratio of MFPTs for  $d$ -dimensional hyper-sphere and 1D sphere (interval), i.e.  $\langle \tau \rangle / \langle \tau \rangle_{d=1} \times d^{\alpha/2}$  (bottom row). Hyper-sphere radius  $R = 5$  (left column) and  $R = 10$  (right column). Various curves correspond to various values of the stability index  $\alpha$ . Lines in the top panel shows theoretical values of the MFPT given by Eq. (24). Error bars in the top panel are smaller than the symbol size.

infinite second moment

$$\langle x^2 \rangle = \int_{-\infty}^{\infty} x^2 l_{\alpha,0}(x) dx = \infty, \quad (26)$$

where  $l_{\alpha,0}$  is the symmetric 1D  $\alpha$ -stable density with the characteristic function given by Eq. (3). Nevertheless, in practical realizations empirical second moment grows like a power-law, due to effective cut-off of the distribution support. A nice explanation of this fact comes from Bouchaud and Georges [52] and is repeated in [53]. Among  $N$  performed jumps there is the largest one, let say  $l_c(N)$ , whose length grows like

$$l_c(N) \propto N^{1/\alpha}. \quad (27)$$

Eq. (27) gives effective threshold for the support of distribution. Using Eq. (27) and an asymptotic form of symmetric  $\alpha$ -stable densities

$$l_{\alpha,0}(x) \propto |x|^{-(1+\alpha)}, \quad (28)$$

it is possible to estimate  $\langle x^2 \rangle$  as

$$\langle x^2 \rangle \approx \int^{l_c} x^2 l_{\alpha,\beta}(x) dx \approx \left(N^{1/\alpha}\right)^{2-\alpha} = N^{2/\alpha-1}. \quad (29)$$

After  $N$  jumps

$$\langle x^2 \rangle_N = N \langle x^2 \rangle \propto N^{2/\alpha} \propto t^{2/\alpha}, \quad (30)$$

because jumps are performed every  $\Delta t$ . Consequently, for Lévy flights (sample based) standard deviation grows like a power law with the number of jumps  $N$  (time  $t$ ).

Escape from the interval takes place when characteristic width of distribution of position  $x$  is equal to the interval half-width  $R$ . More precisely when

$$R^2 \approx \langle x^2 \rangle. \quad (31)$$

In  $d$  dimensions instead of  $\langle x^2 \rangle$  one needs to calculate  $\langle \mathbf{x}^2 \rangle$ . Assuming that jumps along axis are independent

$$\langle \mathbf{x}^2 \rangle = \langle x_1^2 \rangle + \dots + \langle x_d^2 \rangle = d \times \langle x^2 \rangle \propto d \times t^{2/\alpha}. \quad (32)$$

A random walker escapes the hyper-sphere when

$$R^2 \approx d \times t^{2/\alpha}. \quad (33)$$

Therefore, the escape time scales as

$$\mathcal{T} \propto \frac{R^\alpha}{d^{\alpha/2}}. \quad (34)$$

The above considerations assume that jumps along all axis are independent, what is not the case of general multi-variate  $\alpha$ -stable densities with  $\alpha < 2$ , see [30]. Nevertheless, the scaling (34) holds for all simulations performed, see bottom panel of Fig. 4, which presents the ratio of MFPTs for  $d$ -dimensional hyper-sphere and 1D sphere (interval), i.e.  $\langle \tau \rangle / \langle \tau \rangle_{d=1} \times d^{\alpha/2}$ . Some deviation from the theoretical scaling are visible for  $\alpha \approx 2$  and small  $R$ , e.g.  $R = 5$ . These discrepancies originate in some inaccuracies of simulations of escape from highly dimensional small hyper-spheres. Nevertheless, as it can be seen in the top panel of Fig. 4, the MFPT clearly follows the  $d^{-\alpha/2}$  scaling. This can be further confirmed by fits, which only for clarity of the figure are not depicted in the top panel of Fig. 4, perfectly following  $d^{-\alpha/2}$  scaling predicted by Eq. (34).

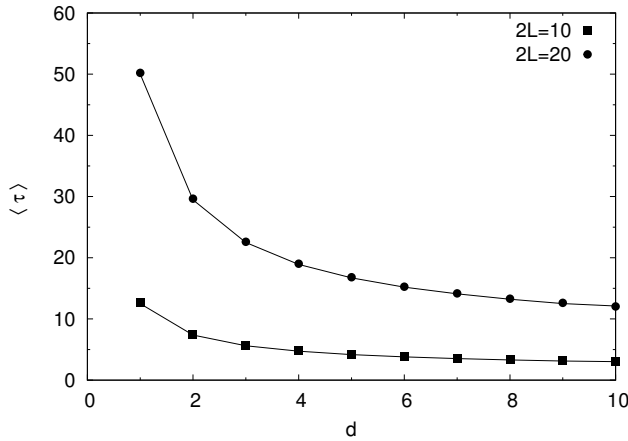


FIG. 5: Mean first passage time for escape from  $d$ -dimensional hyper-cube for  $\alpha = 2$ . Points represents results of numerical simulations while solid lines present theoretical values. Error bars are smaller than the symbol size.

## 2. Hyper-cube

Analogously like in 1D, in  $d$ -dimensions, for the Gaussian case ( $\alpha = 2$ ) the solution of diffusion equation

$$\frac{\partial p(\mathbf{x}, t | \mathbf{x}_0, 0)}{\partial t} = \nabla^2 p(\mathbf{x}, t | \mathbf{x}_0, 0) \quad (35)$$

can be constructed using Fourier series [42, Eq. (81)] and for  $\mathbf{x}_0 = \mathbf{0}$ , it reads

$$p(\mathbf{x}, t | \mathbf{0}, 0) = \sum_{\{i_1, \dots, i_d\}=1}^{\infty} \frac{1}{L^d} \sin \left[ \frac{i_1 \pi}{2} \right] \sin \left[ \frac{i_1 \pi (x_1 + L)}{2L} \right] \times \dots \times \sin \left[ \frac{i_d \pi}{2} \right] \sin \left[ \frac{i_d \pi (x_d + L)}{2L} \right] \exp \left[ -\frac{\pi^2 \sigma^2}{4L^2} (i_1^2 \dots i_d^2) t \right]. \quad (36)$$

From Eq. (36) one gets the survival probability

$$S(t) = \frac{4^d}{\pi^d} \sum_{\{i_1, \dots, i_d\}=1}^{\infty} \frac{\sin [i_1 \pi / 2]}{i_1} \times \dots \times \frac{\sin [i_d \pi / 2]}{i_d} \exp \left[ -\frac{\pi^2 \sigma^2}{4L^2} (i_1^2 + \dots + i_d^2) t \right]. \quad (37)$$

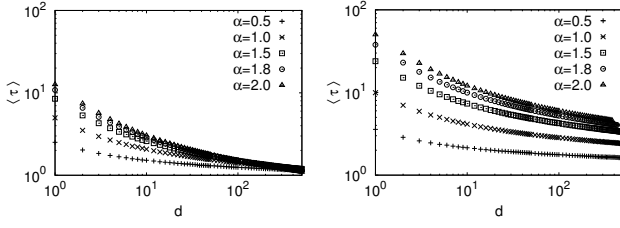


FIG. 6: The mean first passage times  $\langle \tau \rangle$  for the escape from the  $d$ -dimensional hyper-cube. The hyper-cube's edge  $2L = 10$  (left panel) and  $2L = 20$  (right panel), i.e. the hyper-cube edge is the same as the hyper-sphere diameter in Fig. 4. Various curves correspond to various values of the stability index  $\alpha$ . Error bars are smaller than the symbol size.

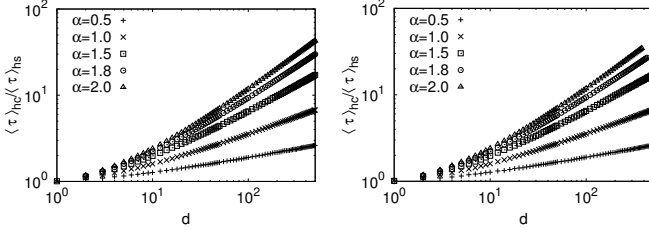


FIG. 7: The ratio of mean first passage times  $\langle \tau \rangle$  for escape from  $d$ -dimensional hyper-cube and  $d$ -dimensional hyper-sphere. Hyper-sphere radius  $R = 5$  (left panel) and  $R = 10$  (right panel). The hyper-cube edge is equal to the hyper-sphere diameter. Various curves correspond to various values of the stability index  $\alpha$ .

Finally, the formula for the mean first passage time takes the form

$$\mathcal{T} = \langle \tau \rangle = \int_0^\infty S(t) dt = \frac{4^{d+1} L^2}{\pi^{2+d} \sigma^2} \sum_{\{i_1, \dots, i_d\}=1}^\infty \frac{\sin[i_1 \pi/2]}{i_1} \times \dots \times \frac{\sin[i_d \pi/2]}{i_d} \frac{1}{i_1^2 + \dots + i_d^2}. \quad (38)$$

The above formula can be approximated by combinational methods. The dominating contribution comes from small values of indices, e.g. when they are equal to  $\{1, 3, 5, 7, 9\}$  and they are repeated  $d - k - l - m - n$ ,  $k$ ,  $l$ ,  $m$  and  $n$  times respectively, consequently

$$\mathcal{T} \approx \frac{4^{d+1} L^2}{\pi^{2+d} \sigma^2} \sum_{\{k, l, m, n\}=1}^{k+l+m+n \leq d} \frac{d!}{(d-k-l-m-n)! k! l! m! n!} \times \frac{(-1)^{k+m}}{3^k \times 5^l \times 7^m \times 9^n} \times \frac{1}{3^2 k + 5^2 l + 7^2 m + 9^2 n + d - k - l - m - n}. \quad (39)$$

The combinational factor indicates the fact that summed elements do not depend on the order of indices. The second term is due to the product of  $\sin[i\pi/2]/i$  terms. Finally, the last term is  $(i_1^2 + \dots + i_d^2)^{-1}$ . MFPTs from stochastic simulations along with the approximation given by Eq. (39) are presented in Fig. 5. The mean first passage time is proportional to  $L^2/\sigma^2$  for all dimensions  $d$ . For  $d = 1$ , the standard formula is recovered, see Eq. (8). For the hyper-cube with  $\alpha = 2$ , the MFPT calculated according to Eq. (39) perfectly agrees with simulations, see Fig. 5. Theoretical values of the MFPT are depicted by solid lines which have interpretation for integer  $d$  only and the rest of curves is drawn to guide the eye only. In analogy to the Gaussian case, for  $\alpha < 2$ , the MFPT is proportional to  $L^\alpha/\sigma^\alpha$ .

Figure 6 presents the mean first passage time from the  $d$ -dimensional hyper-cube as a function of the dimension  $d$ . Various curves correspond to various values of the stability index  $\alpha$ . As it can be deduced from comparison of Figs. 4 and 6 the noise induced escape from the hyper-sphere is faster than escape from the hyper-cube because average distance to the absorbing boundary is smaller for the hyper-sphere than the hyper-cube. This is further corroborated by Fig. 7 which presents the ratio of mean first passage times from hyper-spheres and hyper-cubes. The parameters are chosen in such a way that the hyper-sphere diameter is equal to the hyper-cube edge. For the hyper-sphere the MFPT decreases like a power-law with increasing dimension  $d$ , see Fig. 6 and Eq. (34). For the hyper-cube the dependence is not of the power-law type, see Fig. 6, and follow more complex pattern.

Escape from the hyper-cube can be used to verify if increments of the  $L_\alpha(t)$  process along various directions are independent and identically distributed. If axis are perpendicular to walls of the hyper-cube and jumps along axis are independent identically distributed, escape from the hyper-cube is equivalent to the first order statistics of  $d$   $L_{\alpha,0}(t)$  processes. More precisely, in  $d$  dimensions if all components of  $L_\alpha(t)$  are independent, one can calculate  $d$  first passage times  $\tau_1, \dots, \tau_d$ , where  $\tau_i$  represents exit time from interval  $[-L, L]$  of the  $i$ -th component of  $L_\alpha(t)$ . Since the hyper-cube is  $[-L, L] \times \dots \times [-L, L]$  and components of  $L_\alpha(t)$  are independent, the first exit from the hyper-cube takes place for  $\tau = \min\{\tau_1, \dots, \tau_d\}$ , which is the minimal first exit time, i.e. the first order statistics [54, 55]. Additionally, if jumps' components are identically distributed, the survival probability is  $S_d^{\min}(t) = [S_1(t)]^d = S_d(t)$ , where  $S_1(t)$  is the survival probability for the escape from  $[-L, L]$  interval and  $S_d(t)$  is the survival probability for escape from  $d$  dimensional hyper-cube. Consequently, if components of  $L_\alpha(t)$  are independent, identically distributed  $[S_d(t)]^{1/d}$  with various  $d$  should coincide. Indeed, that is the case for  $\alpha = 2$ , while for  $\alpha < 2$  they differ, see Fig. 8. For  $\alpha = 2$ , if covariance matrix is proportional to the identity matrix, the  $L_2(t)$  process has independent components, what is not necessarily the case for  $\alpha < 2$ . The disagreement of  $[S_d(t)]^{1/d}$  for  $\alpha < 2$  is due to the fact, that  $L_\alpha(t)$  represents here the  $\alpha$ -stable random vector with the uniform spectral measure. In such a case, components of the vector are dependent, see [30], and the escape from the hyper-cube cannot be seen as the escape from Cartesian product of  $d$   $[-L, L]$  intervals, because jump components are no longer independent identically distributed. Nevertheless, it is still possible to consider  $L_\alpha(t)$  processes with symmetric discrete spectral measures concentrated on intersections of axes with the unit hyper-sphere. Such a process has independent identically distributed increments, see [30, Example 2.3.5], and consequently the property  $[S_d(t)]^{1/d} = S_1(t)$  holds (results not shown), however probability densities of such processes are not spherically symmetric.

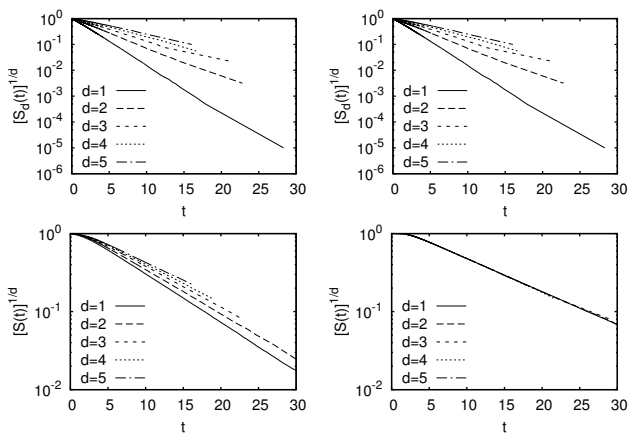


FIG. 8: Rescaled survival probabilities  $[S_d(t)]^{1/d}$  for various values of the stability index  $\alpha$ :  $\alpha = 0.5$  (left-top),  $\alpha = 1.0$  (right-top),  $\alpha = 1.5$  (left-bottom) and  $\alpha = 2$  (right-bottom). Various lines represent various dimension  $d$ . The hyper-cube edge is  $2L = 10$ .

### III. SUMMARY AND CONCLUSIONS

White  $\alpha$ -stable noise provides a natural generalization of white Gaussian noise including the latter as a special limiting case of  $\alpha = 2$ . One dimensional  $\alpha$ -stable noises are characterized by four parameters. Consequently, systems driven by  $\alpha$ -stable noise can display richer behavior than their Gaussian white noise driven counterparts. One of such examples is an escape problem from the finite interval restricted by two absorbing boundaries. If the escape is driven by Gaussian white noise, the mean first passage time depends on the interval width, initial position and the noise intensity. In general the MFPT decreases with the increase of the noise intensity because large noise intensity enhances probability of longer jumps.

The very different situation takes place when the escape process is driven by  $\alpha$ -stable noise. If the noise is symmetric, the mean first passage time is not only characterized by the scale parameter  $\sigma$  but also by a stability index  $\alpha$ . As in the white Gaussian noise driven escape, the MFPT decreases with the increase of scale parameter. However, for appropriate choice of parameters, the MFPT can be non-monotonous function of the stability index due to interplay between noise parameters.

Within the current manuscript noise driven escape from bounded domains has been studied in order to verify if the non-monotonous dependence of the mean first passage time on the stability index is observed in higher-dimensions. As a basic setup the escape from the disk has been considered. Extensive numerical simulations have corroborated the possibility of non-monotonous dependence of the MFPT on the stability index  $\alpha$  when the whole disk edge or a part of the disk edge are absorbing.

Noise driven escape from hyper-spheres and hyper-cubes have been considered as well. The escape process from the hyper-sphere is faster than the escape process from the hyper-cube despite the fact that hyper-cube's edge is equal to the hyper-sphere's diameter. With the increasing number of dimension the mean first passage time decreases revealing an apparent power-law scaling with the dimension  $d$  for escape from the hyper-sphere. The escape time from the hyper-cube decreases with the increase of dimension  $d$  according to more complex pattern. Finally, the noise induced escape from the hyper-cube can be used to recognize if the noise induced increments are independent.

In general the problem of multi-variate noise induced escape provides a challenging task due to properties of multi-variate  $\alpha$ -stable noises. In 1D parameters characterizing  $\alpha$ -stable noises have clear and intuitive interpretation. In the multi-variate case main characteristics of  $\alpha$ -stable noises are determined by properties of the spectral measure. Various spectral measures results in various escape scenarios. Here, we have focused on a uniform continuous spectral measure as the one leading to spherically symmetric jumps length distributions.

### Acknowledgments

Computer simulations have been performed at the Academic Computer Center Cyfronet, Akademia

Górniczno-Hutnicza (Kraków, Poland) under CPU grant MNiSW/Zeus\_lokalnie/UJ/052/2012.

- 
- [1] E. W. Montroll and G. H. Weiss, *J. Math. Phys.* **6**, 167 (1965).
- [2] E. W. Montroll and M. F. Shlesinger, in *Lévy processes: Theory and applications*, edited by J. L. Lebowitz and E. W. Montroll (North Holland, Amsterdam, 1984), pp. 1–121.
- [3] R. Metzler and J. Klafter, *Phys. Rep.* **339**, 1 (2000).
- [4] M. F. Shlesinger, *J. Chem. Phys.* **78**, 416 (1983).
- [5] R. Metzler and J. Klafter, *J. Phys. A: Math. Gen.* **37**, R161 (2004).
- [6] F. Bartumeus, M. G. E. da Luz, G. M. Viswanathan, and J. Catalan, *Ecology* **86**, 3078 (2005).
- [7] M. Esposito and K. Lindenberg, *Phys. Rev. E* **77**, 051119 (2008).
- [8] E. Scalas, *Physica A* **362**, 225 (2006).
- [9] E. Abad, S. B. Yuste, and K. Lindenberg, *Phys. Rev. E* **81**, 031115 (2010).
- [10] A. Bar-Haim and J. Klafter, *J. Chem. Phys.* **109**, 5187 (1998).
- [11] T. H. Solomon, E. R. Weeks, and H. L. Swinney, *Phys. Rev. Lett.* **71**, 3975 (1993).
- [12] T. H. Solomon, E. R. Weeks, and H. L. Swinney, *Physica D* **76**, 70 (1994).
- [13] A. V. Chechkin, V. Y. Gonchar, and M. Szydlowski, *Phys. Plasmas* **9**, 78 (2002).
- [14] S. Boldyrev and C. R. Gwinn, *Phys. Rev. Lett.* **91**, 131101 (2003).
- [15] M. F. Shlesinger, G. M. Zaslavsky, and J. Frisch, eds., *Lévy flights and related topics in physics* (Springer Verlag, Berlin, 1995).
- [16] O. E. Barndorff-Nielsen, T. Mikosch, and S. I. Resnick, eds., *Lévy processes: Theory and applications* (Birkhäuser, Boston, 2001).
- [17] P. D. Ditlevsen, *Geophys. Res. Lett.* **26**, 1441 (1999).
- [18] R. N. Mantegna and H. E. Stanley, *An introduction to econophysics. Correlations and complexity in finance* (Cambridge University Press, Cambridge, 2000).
- [19] D. Brockmann, L. Hufnagel, and T. Geisel, *Nature (London)* **439**, 462 (2006).
- [20] B. Dybiec, A. Kleczkowski, and C. A. Gilligan, *J. R. Soc. Interface* **6**, 941 (2009).
- [21] A. V. Chechkin, V. Y. Gonchar, J. Klafter, R. Metzler, and L. V. Tanatarov, *J. Stat. Phys.* **115**, 1505 (2004).
- [22] I. M. Sokolov and V. V. Belik, *Physica A* **330**, 46 (2003).
- [23] A. A. Dubkov, B. Spagnolo, and V. V. Uchaikin, *Int. J. Bifurcation Chaos. Appl. Sci. Eng.* **18**, 2649 (2008).
- [24] M. Rypdal and K. Rypdal, *Phys. Rev. Lett.* **104**, 128501 (2010).
- [25] P. Barthelemy, J. Bertolotti, and D. Wiersma, *Nature (London)* **453**, 495 (2008).
- [26] Z. Pasternak, F. Bartumeus, and F. W. Grasso, *J. Phys. A: Math. Gen.* **42**, 434010 (2009).
- [27] M. A. Lomholt, T. Ambjörnsson, and R. Metzler, *Phys. Rev. Lett.* **95**, 260603 (2005).
- [28] R. Klages, G. Radons, and I. M. Sokolov, *Anomalous transport: Foundations and applications* (Wiley-VCH, Weinheim, 2008).
- [29] A. Janicki and A. Weron, *Simulation and chaotic behavior of  $\alpha$ -stable stochastic processes* (Marcel Dekker, New York, 1994).
- [30] G. Samorodnitsky and M. S. Taqqu, *Stable non-Gaussian random processes: Stochastic models with infinite variance* (Chapman and Hall, New York, 1994).
- [31] O. Benichou, M. Coppey, M. Moreau, P. H. Suet, and R. Voituriez, *Europhys. Lett.* **70**, 42 (2005).
- [32] A. Zoia, A. Rosso, and M. Kardar, *Phys. Rev. E* **76**, 021116 (2007).
- [33] B. Dybiec, *J. Stat. Mech.* p. P01011 (2010).
- [34] B. Dybiec, E. Gudowska-Nowak, and P. Hänggi, *Phys. Rev. E* **73**, 046104 (2006).
- [35] A. M. Edwards, R. A. Phillips, N. W. Watkins, M. P. Freeman, E. J. Murphy, V. Afanasyev, S. V. Buldyrev, M. G. E. da Luz, E. P. Raposo, H. E. Stanley, et al., *Nature (London)* **449**, 1044 (2007).
- [36] M. Teuerle and A. Jurlewicz, *Acta Phys. Pol. B* **40**, 1333 (2009).
- [37] A. Janicki, *Numerical and statistical approximation of stochastic differential equations with non-Gaussian measures* (Hugo Steinhaus Centre for Stochastic Methods, Wrocław, 1996).
- [38] H. C. Fogedby, *Phys. Rev. E* **50**, 1657 (1994).
- [39] R. Metzler, E. Barkai, and J. Klafter, *Europhys. Lett.* **46**, 431 (1999).
- [40] V. V. Yanovsky, A. V. Chechkin, D. Schertzer, and A. V. Tur, *Physica A* **282**, 13 (2000).
- [41] D. Schertzer, M. Larchevêque, J. Duan, V. V. Yanowsky, and S. Lovejoy, *J. Math. Phys.* **42**, 200 (2001).
- [42] D. R. Cox and H. D. Miller, *The theory of stochastic processes* (Chapman and Hall, London, 1965).
- [43] C. W. Gardiner, *Handbook of stochastic methods for physics, chemistry and natural sciences* (Springer Verlag, Berlin, 2009).
- [44] M. Teuerle, P. Żebrowski, and M. Magdziarz, *J. Phys. A: Math. Gen.* **45**, 385002 (2012).
- [45] J. M. Chambers, C. L. Mallows, and B. W. Stuck, *J. Amer. Statistical Assoc.* **71**, 340 (1976).
- [46] R. Weron, *Statist. Probab. Lett.* **28**, 165 (1996).
- [47] J. P. Nolan, in *A practical guide to heavy tails: statistical techniques and applications*, edited by R. J. Feldman and M. S. Taqqu (Birkhäuser, Boston, 1998), p. 509.
- [48] A. V. Chechkin and V. Y. Gonchar, *Open Sys. & Information Dyn.* **7**, 375 (2000).
- [49] S. G. Samko, A. A. Kilbas, and O. I. Marichev, *Fractional integrals and derivatives. Theory and applications.* (Gordon and Breach Science Publishers, Yverdon, 1993).
- [50] A. Singer, Z. Schuss, and D. Holcman, *J. Stat. Phys.* **122**, 465 (2006).
- [51] S. Pillay, M. J. Ward, A. Peirce, and T. Kolokolnikov, *Multi-scale Model. Simul.* **8**, 803 (2010).
- [52] J. P. Bouchaud and A. Georges, *Phys. Rep.* **195**, 127 (1990).
- [53] B. Dybiec and E. Gudowska-Nowak, *Phys. Rev. E* **80**, 061122 (2009).
- [54] H. A. David and H. N. Nagaraja, *Order statistics* (John Wiley, New York, 2003).
- [55] S. B. Yuste, L. Acedo, and K. Lindenberg, *Phys. Rev. E* **64**, 052102 (2001).